Discrete modes of a ferromagnetic stripe dipolarly coupled to a ferromagnetic film: a Brillouin light scattering study

2007 J. Phys.: Condens. Matter 19 246221

(http://iopscience.iop.org/0953-8984/19/24/246221)

IOP PUBLISHING JOURNAL OF PHYSICS: CONDENSED MATTER

J. Phys.: Condens. Matter **19** (2007) 246221 (14pp) doi:10.1088/0953-8984/19/24/246221

Discrete modes of a ferromagnetic stripe dipolarly coupled to a ferromagnetic film: a Brillouin light scattering study

G Gubbiotti[1,7], S Tacchi[2], G Carlotti[2,3], T Ono[4], Y Roussigné[5], V S Tiberkevich[6] and A N Slavin[6]

[1] CNISM, Dipartimento di Fisica, Unità di Perugia, Via A Pascoli, I-06123 Perugia, Italy
[2] Dipartimento di Fisica, Universita' di Perugia, Via A Pascoli, 06123 Perugia, Italy
[3] INFM-CNR Research Center S3, Via Campi 213/a, 41100 Modena, Italy
[4] Institute for Chemical Research, Kyoto University, Uji, Kyoto 611-0011, Japan
[5] CNRS, Laboratoire PMTM, Université Paris 13, 93430 Villetaneuse, France
[6] Department of Physics, Oakland University, Rochester, MI 48309, USA

E-mail: gubbiotti@fisica.unipg.it

Received 3 April 2007, in final form 10 May 2007
Published 25 May 2007
Online at stacks.iop.org/JPhysCM/19/246221

Abstract

Spin wave excitations in a magnetic structure consisting of a series of long permalloy stripes of a rectangular cross section magnetized along the stripe length and situated above a continuous permalloy film are studied both experimentally and theoretically. Stripes and continuous film are coupled by dipole–dipole interaction across 10 nm thick Cu spacers. Experimental measurements made using the Brillouin light scattering technique (with the light wavevector oriented along the stripe width) provide evidence for one dispersive spin wave mode associated with the continuous film and several discrete non-dispersive modes resonating within the finite width of the stripes.

To interpret the experimental spectra, an analytic theory based on the spin wave formalism for finite-width magnetic stripes has been developed, achieving a good qualitative and partly quantitative description of the experimentally observed spin wave spectrum of the system. In particular, it is explained why the presence of a continuous magnetic film near the magnetic stripe leads to a substantial decrease of the frequencies of the discrete dipolar spin wave modes localized within the stripes. A more quantitative description of the measured frequencies and of the spatial profiles of the spin wave eigenmodes has been obtained by numerical calculations performed using a finite element method.

(Some figures in this article are in colour only in the electronic version)

[7] Author to whom any correspondence should be addressed.

1. Introduction

The study of spin dynamics in laterally patterned magnetic structures is an interesting and challenging research field. Its development started about a decade ago when advances in lithography made possible the realization of patterns of nanometric magnetic elements with controlled lateral shape and dimensions. Ordered arrays of long magnetic stripes with micrometric width served as a model system to shed light on the new properties of spin wave excitations in laterally confined magnetic elements. These new properties arise both from the boundary conditions for the dynamical magnetization at the lateral edges of magnetic elements and from the inhomogeneity of the dipolar demagnetizing field associated to the particular shape of the magnetic elements.

The first studies were performed on stripe arrays with relatively large distances between stripes, when the dipole–dipole interaction between stripes was negligible [1]. In that case, the frequency spectrum of an array of stripes, measured as a function of the in-plane wave number, coincides with that of a single stripe. It consists of several dispersionless branches corresponding to spin wave modes standing along the stripe width. Later, experimental and theoretical investigations were performed on arrays of closely spaced magnetic stripes, in which dipole–dipole interaction between stripes was important, and a collective spin wave mode of the whole array with a continuous frequency spectrum was found in a certain range of frequencies [2, 3].

Another interesting system in which the influence of dipolar coupling between elements on the spin wave spectrum of the system can be studied experimentally is the system of layered nanometric elements having layers of different magnetic materials separated by non-magnetic spacers with thickness in the nanometric range. The principal effect of the magnetic dipolar coupling between the layers is the formation of 'acoustic' (in-phase) and 'optic' (in anti-phase) coupled spin wave modes in layered structures and the consequent substantial modification of the spin wave spectrum in a multi-layer array compared to an array of single-layer elements of the same size [4–10].

In this paper we study both experimentally and theoretically the spectrum of collective spin wave modes in an array of long magnetic stripes which are situated over a continuous magnetic film, with a Cu interlayer, so that intensive dipole–dipole interaction between the stripes and the film takes place. At the same time, the lateral separation between the stripes was chosen to be large enough to exclude the dipole–dipole interaction between stripes. The stripes were magnetized along their length (easy magnetization direction), so the demagnetizing field is negligible and the static magnetic field inside the stripe homogeneous.

The paper has the following structure: in section 2 the details about the sample fabrication are presented together with the experimental techniques; sections 3 and 4 are devoted to the description of our analytical and numerical calculations, respectively, while in section 5 the comparison between the experimental and theoretical results is discussed.

2. Sample preparation and experimental results

The studied sample consists of an array of patterned $Ni_{80}Fe_{20}$ (30 nm)/Cu (10 nm) stripes, having width $w = 0.5\ \mu$m and lateral spacing $s = 0.5\ \mu$m, deposited on top of a continuous (unpatterned) permalloy film 30 nm thick. The layered structure, shown in figure 1, was fabricated on thermally oxidized Si substrates by means of electron-beam lithography, electron-gun deposition, and a lift-off process. The stripes were arranged in arrays of dimensions of $800 \times 800\ \mu m^2$. A similar array of single-layer isolated permalloy stripes was also fabricated and used as a reference sample.

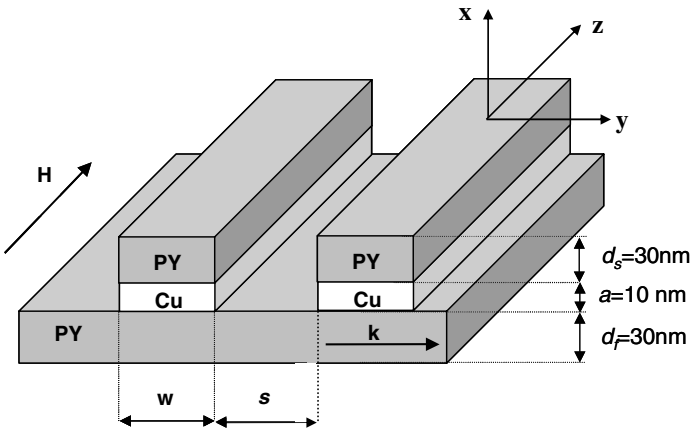

Figure 1. Schematic representation of the sample structure. NiFe (30 nm)/Cu (10 nm) stripes, 0.5 μm wide, are fabricated on a 30 nm thick NiFe sublayer and their separation is $s = 0.5$ μm. An external magnetic field H is applied parallel to the long axis of the stripes.

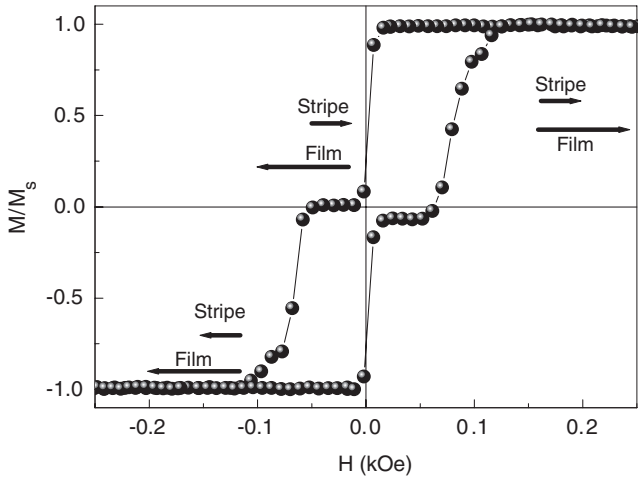

Figure 2. Hysteresis loop of the array of NiFe/Cu stripes on a NiFe sublayer measured by the MOKE technique in the longitudinal configuration. The arrows indicate the orientation of the stripes and film magnetizations at different values of the external magnetic field H.

The hysteresis loops of the sample were measured by the specular magneto-optic Kerr effect (MOKE) technique in the longitudinal configuration, i.e., with the external field applied parallel to the long axis of the stripes (along the 'easy' direction of magnetization). The method of nearly crossed polarizer [11], which employs an amplitude-modulated laser with modulation frequency of 450 Hz and a lock-in amplifier, was used in our experiments.

The measured hysteresis loop of our sample is shown in figure 2. As shown by the arrows in figure 2, the cycle is characterized by a plateau corresponding to the antiparallel alignment of the magnetizations of the stripes and the permalloy film, stabilized by the dipolar coupling between them. This coupling favours the closure of the magnetic flux through the permalloy layers. The MOKE signal comes from the portion of the sample which is directly illuminated by light; because of the attenuation depth of light the film beyond the stripes is not reached.

Therefore, the drop in the magnetization curve observed when H is reversed is proportional to the ratio between the width of the stripes (w) and the period of the structure (stripes plus continuous film directly illuminated by light: $T = w + \Delta$). In our case we expect a drop of 50%, which is in good agreement with the experimental value.

The frequency spectra of the spin wave excitations were measured by the Brillouin light scattering (BLS) technique. The BLS experiments were carried out at the GHOST laboratory [12], Perugia University, using a Sandercock (3 + 3)-pass tandem Fabry–Perot interferometer [13]. The light source used in the BLS experiments is a single-mode solid state laser operating at $\lambda = 532$ nm with the output power of 250 mW. A camera objective of f-number 2 and focal length 50 mm is used to focus light onto the sample surface. The scattered light was sent through a crossed analyser to suppress the background of elastically scattered light and the signal from surface phonons. The sample was mounted on a goniometer to allow rotation around the field direction, i.e. to vary the incidence angle of light (θ) between 10° and 70°. The spin wave wavevector probed is parallel to the wire width (y-direction) and its magnitude, ranging from 0.41×10^5 to 2.22×10^5 cm^{-1}, is related to the angle of incidence by $k = (4\pi/\lambda)\sin\theta$. The scheme of the sample and the experimental geometry, showing the orientation of the applied field H and the direction of the wavevector k, is shown in figure 1 together with the orientation of the Cartesian coordinate system used for the following calculations.

The spectra of normal spin wave modes of the sample were recorded in two different types of measurement: (i) by changing the transferred in-plane wavevector k (contained in the x–y plane) at a fixed value of the bias magnetic field $H = 300$ Oe applied parallel to the long side of the wires (z-direction), and (ii) by changing the magnitude of H in the range between +300 and −300 Oe at a fixed value ($\theta = 54°$ and therefore $k = 1.91 \times 10^5$ cm^{-1}) of the incidence angle of light.

Two representative BLS spectra, recorded in the same experimental conditions ($H = 0.3$ kOe applied along the stripes long axis and incidence angle of $\theta = 30°$), are presented in figure 3 for arrays of isolated stripes *(a)* (reference sample) and those deposited on the continuous permalloy layer *(b)* (main sample). We note that, even though a large number of well resolved peaks are seen in both spectra, the main effect of the presence of the continuous permalloy layer in the vicinity of the stripe array is the substantial reduction of the mode frequencies. They are located in the interval between 8.5 and 16 GHz for the isolated array of stripes (figure 3*(a)*), while the interval shifts down between 6 and 13 GHz for the array of stripes deposited on the permalloy sublayer (figure 3*(b)*).

3. Analytical model

To explain the above-mentioned decrease of spin wave mode frequencies in the case when dipole–dipole interaction between the stripe array and the continuous magnetic film takes place we developed the following analytical model. We took a linearized Landau–Lifshitz equation of motion and wrote it for the variable magnetizations of the film $\mathbf{m}_\mathrm{f}$ and stripe $\mathbf{m}_\mathrm{s}$, assuming that interaction between the stripes is negligible:

$$\dot{\mathbf{m}}_\mathrm{f} = \left[(\omega_H - \omega_M \alpha \Delta)\,\hat{\mathbf{z}} \times \mathbf{m}_\mathrm{f}\right] - \gamma M_\mathrm{S}\left[\hat{\mathbf{z}} \times \left(\mathbf{h}_{\mathrm{f,f}} + \mathbf{h}_{\mathrm{f,s}}\right)\right] \tag{1a}$$

$$\dot{\mathbf{m}}_\mathrm{s} = \left[(\omega_H - \omega_M \alpha \Delta)\,\hat{\mathbf{z}} \times \mathbf{m}_\mathrm{s}\right] - \gamma M_\mathrm{S}\left[\hat{\mathbf{z}} \times \left(\mathbf{h}_{\mathrm{s,s}} + \mathbf{h}_{\mathrm{s,f}}\right)\right]. \tag{1b}$$

Here $\omega_H = \gamma H$, $\omega_M = 4\pi\gamma M_\mathrm{s}$, H is the bias magnetic field, γ is the gyromagnetic ratio, M_s is the saturation magnetization, $\alpha = A/2\pi M_\mathrm{S}^2$, where A is the exchange constant measured in erg cm^{-1}, Δ is the Laplace operator, and $\mathbf{h}_{\mathrm{f,s}}$ and $\mathbf{h}_{\mathrm{f,f}}$ are the variable dipolar magnetic fields, created by the film dynamic magnetization $\mathbf{m}_\mathrm{f}$ in the stripe and the film itself, respectively.

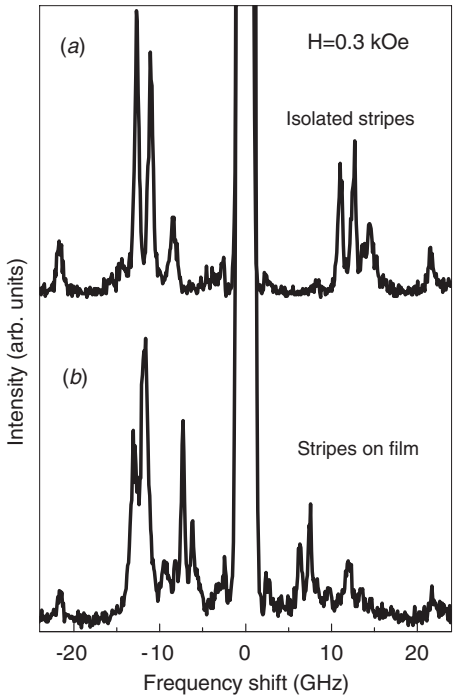

Figure 3. Brillouin light scattering spectra recorded for an applied field of 0.3 kOe for *(a)* the reference sample: an array of isolated NiFe stripes and *(b)* the main sample: an array the NiFe/Cu stripes on a NiFe sublayer.

Similarly, $\mathbf{h}_{\mathrm{s,s}}$ and $\mathbf{h}_{\mathrm{s,f}}$ are the corresponding fields created by the dynamic magnetization of the stripe. The magnetizations $\mathbf{m}_{\mathrm{f,s}}$ are orthogonal to the constant magnetization $M_{\mathrm{s}}\hat{\mathbf{z}}$, i.e. they have only x and y components, $\mathbf{m}_{\mathrm{f,s}} = m^{x}_{\mathrm{f,s}}\hat{\mathbf{x}} + m^{y}_{\mathrm{f,s}}\hat{\mathbf{y}}$. In the considered case of thin ferromagnetic layers, the exchange splitting $\approx\omega_M\alpha_{\mathrm{ex}}/d^2_{\mathrm{s,f}}$ between the different thickness modes will be so large that they are almost fully decoupled. Considering only the lowest (quasi-uniform) thickness mode and assuming the free (unpinned) surface spins at the vertical (normal to the x-axis) boundaries of the ferromagnetic layers, one can assume that the magnetizations $\mathbf{m}_{\mathrm{f,s}}$ depend only on the y coordinate.

The dipolar magnetic fields $\mathbf{h}_{\mathrm{f,s}}$ in equation (1) are treated as the averaged (over the thickness of the corresponding ferromagnetic layer) values of the real magnetic fields. The magnetization $\mathbf{m}_{\mathrm{f}}$ of the magnetic film can be developed in a Fourier series as

$$\mathbf{m}_{\mathrm{f}}(t, y) = \int_{-\infty}^{\infty} \mathbf{m}_{\mathrm{fk}}(t)\mathrm{e}^{\mathrm{i}ky}\frac{\mathrm{d}k}{2\pi} \tag{2}$$

where $\mathbf{m}_{\mathrm{fk}} = \mathbf{m}^{*}_{f-k}$. The dipolar field created by the magnetization (2), averaged over the thickness of the film, is given by

$$\mathbf{h}_{\mathrm{ff}} = -4\pi\int_{-\infty}^{\infty}\frac{\mathrm{d}k}{2\pi}\mathrm{e}^{\mathrm{i}ky}\left\{P(kd_{\mathrm{f}})\,m^{x}_{\mathrm{fk}}\hat{\mathbf{x}} + [1 - P(kd_{\mathrm{f}})]\,m^{y}_{\mathrm{fk}}\hat{\mathbf{y}}\right\} \tag{3}$$

where

$$P(\xi) = \frac{1 - \mathrm{e}^{-|\xi|}}{|\xi|} \tag{4}$$

while the dipolar field averaged over the thickness of the stripe has the form

$$\mathbf{h}_{\mathrm{s,f}} = 2\pi \int_{-\infty}^{\infty} \frac{\mathrm{d}k}{2\pi} \mathrm{e}^{\mathrm{i}ky} \left\{ |k|\, d_{\mathrm{f}} Q_k \left(m_{\mathrm{fk}}^x - \mathrm{i}\,\mathrm{sgn}\,(k)\, m_{\mathrm{fk}}^y \right) \left(\hat{\mathbf{x}} - \mathrm{i}\,\mathrm{sgn}\,(k)\, \hat{\mathbf{y}} \right) \right\} \tag{5}$$

where

$$Q_k = \mathrm{e}^{-|k|a} P\,(kd_{\mathrm{f}})\, P\,(kd_{\mathrm{s}}) \tag{6}$$

and a is the thickness of the non-magnetic spacer.

The magnetization in the ferromagnetic stripe $\mathbf{m}_{\mathrm{s}}$ can be written as

$$\mathbf{m}_{\mathrm{s}}\,(t, y) = \sum_{n=0} \sqrt{\frac{w}{w_n}} \mathbf{m}_{sn}\,(t) \sin\,(\beta_n y + \phi_n) \tag{7}$$

where β_n and ϕ_n are determined by the boundary conditions for spins at the lateral edges of the stripe [14], and w_n are the normalization constants, defined by

$$\int_0^w \sin\,(\beta_n y + \phi_n) \sin\,(\beta_m y + \phi_m)\, \mathrm{d}y = w_n \delta_{nm}. \tag{8}$$

To find the dipolar field created by the magnetization $\mathbf{m}_{\mathrm{s}}$ we note that the magnetization, given by equation (7) in the region $0 < y < w$ and vanishing everywhere else, can be written as

$$\mathbf{m}_{\mathrm{s}} = \int_{-\infty}^{\infty} \sum_{n=0}^{\infty} Y_{kn} \mathbf{m}_{sn} \mathrm{e}^{\mathrm{i}ky} \frac{\mathrm{d}k}{2\pi} \tag{9}$$

where

$$Y_{kn} = \sqrt{\frac{w}{w_n}} \int_0^w \sin\,(\beta_n y + \phi_n)\, \mathrm{e}^{-\mathrm{i}ky} \mathrm{d}y = \frac{\sqrt{w/w_n}}{\beta_n^2 - k^2} \Big\{ \beta_n \cos\phi_n + \mathrm{i}k \sin\phi_n - \mathrm{e}^{-\mathrm{i}kw} \left[\beta_n \cos\,(\beta_n w + \phi_n) + \mathrm{i}k \sin\,(\beta_n w + \phi_n) \right] \Big\}. \tag{10}$$

Then the dipolar magnetic field averaged over the thickness of the stripe can be written as

$$\mathbf{h}_{\mathrm{ss}} = -4\pi \sum_{n=0}^{\infty} \int_{-\infty}^{\infty} \frac{\mathrm{d}k}{2\pi} \mathrm{e}^{\mathrm{i}ky} Y_{kn} \left\{ P\,(kd_{\mathrm{s}})\, m_{\mathrm{sk}}^x \hat{\mathbf{x}} + (1 - P\,(kd_{\mathrm{s}}))\, m_{\mathrm{sk}}^y \hat{\mathbf{y}} \right\} \tag{11}$$

while the magnetic field, averaged over the thickness of the film, has the form

$$\mathbf{h}_{\mathrm{fs}} = 2\pi \sum_{n=0}^{\infty} \int_{-\infty}^{\infty} \frac{\mathrm{d}k}{2\pi} \mathrm{e}^{iky} Y_{kn} \left\{ |k|\, d_{\mathrm{s}} Q_k \left(m_{\mathrm{sk}}^x + \mathrm{i}\,\mathrm{sgn}\,(k)\, m_{\mathrm{sk}}^y \right) \left(\hat{\mathbf{x}} + \mathrm{i}\,\mathrm{sgn}\,(k)\, \hat{\mathbf{y}} \right) \right\}. \tag{12}$$

Substituting the expressions (2) and (7) for $\mathbf{m}_{\mathrm{f}}$ and $\mathbf{m}_{\mathrm{s}}$ in the Landau–Lifshitz equation (1), using the expressions for the dipolar fields equations (3), (5), (11), and (12), and the orthogonality conditions, equation (8), one derives equations for the Fourier amplitudes of the variable magnetizations in the film $\mathbf{m}_{\mathrm{fk}}$ and the stripe $\mathbf{m}_{sn}$:

$$\dot{m}_{\mathrm{fk}}^x = -A_k m_{\mathrm{fk}}^y + \mathrm{i}\frac{\omega_M}{2} k d_{\mathrm{s}} Q_k \sum_{n=0}^{\infty} Y_{kn} \left(m_{sn}^x + \mathrm{i}\,\mathrm{sgn}\,(k)\, m_{sn}^y \right) \tag{13a}$$

$$\dot{m}_{\mathrm{fk}}^y = B_k m_{\mathrm{fk}}^x - \mathrm{i}\frac{\omega_M}{2} k d_{\mathrm{s}} Q_k \sum_{n=0}^{\infty} Y_{kn} \left(m_{sn}^y - \mathrm{i}\,\mathrm{sgn}\,(k)\, m_{sn}^x \right) \tag{13b}$$

$$\dot{m}_{sn}^x = -\left(\omega_{Hn} + \omega_M\right) m_{sn}^y + \omega_M \sum_{n=0}^{\infty} P_{nn'} m_{sn'}^y - \mathrm{i}\frac{\omega_M}{2L} \int_{-\infty}^{\infty} \left\{ Y_{kn}^* k d_{\mathrm{f}} Q_k \left(m_{\mathrm{fk}}^x - \mathrm{i}\,\mathrm{sgn}\,(k)\, m_{\mathrm{fk}}^y \right) \right\} \frac{\mathrm{d}k}{2\pi} \tag{13c}$$

$$\dot{m}_{sn}^y = \omega_{Hn} m_{sn}^x + \omega_M \sum_{n=0}^{\infty} P_{nn'} m_{sn'}^x + \mathrm{i}\frac{\omega_M}{2L} \int_{-\infty}^{\infty} \left\{ Y_{kn}^* k d_{\mathrm{f}} Q_k \left(m_{\mathrm{fk}}^y + \mathrm{i}\,\mathrm{sgn}\,(k)\, m_{\mathrm{fk}}^x \right) \right\} \frac{\mathrm{d}k}{2\pi}. \tag{13d}$$

Here

$$A_k = \omega_{Hk} + \omega_M \left(1 - P\left(kd_\mathrm{f}\right)\right) \tag{14a}$$

$$B_k = \omega_{Hk} + \omega_M P\left(kd_\mathrm{f}\right) \tag{14b}$$

$$\omega_{Hk} = \omega_H + \omega_M \alpha k^2 \tag{14c}$$

$$\omega_{Hn} = \omega_H + \omega_M \alpha \beta_n^2 \tag{14d}$$

$$P_{nn'} = \frac{1}{L}\int_{-\infty}^{\infty} P\left(kd_\mathrm{f}\right) Y_{kn}^{*} Y_{kn'} \frac{\mathrm{d}k}{2\pi}. \tag{14e}$$

A monochromatic particular solution of the system of equations (13) can be found by replacing $\mathrm{d}/\mathrm{d}t$ with $-\mathrm{i}\omega$. Solving equations (13*a*) and (13*b*), one can find the components in the film magnetization:

$$m_{\mathrm{fk}}^{x} = \frac{\omega_M}{2} k d_\mathrm{s} Q_k \frac{\omega + \mathrm{sgn}\left(k\right) A_k}{\omega_k^2 - \omega^2} \sum_{n=0}^{\infty} Y_{kn}\left(m_{sn}^{x} + \mathrm{i}\,\mathrm{sgn}\left(k\right) m_{sn}^{y}\right) \tag{15a}$$

$$m_{\mathrm{fk}}^{y} = \mathrm{i}\frac{\omega_M}{2} k d_\mathrm{s} Q_k \frac{B_k + \mathrm{sgn}\left(k\right)\omega}{\omega_k^2 - \omega^2} \sum_{n=0}^{\infty} Y_{kn}\left(m_{sn}^{x} + \mathrm{i}\,\mathrm{sgn}\left(k\right) m_{sn}^{y}\right). \tag{15b}$$

Here ω_k is the frequency of the surface spin wave mode with wavevector k propagating in the film in the y-direction (similar to the Damon–Eshbach mode [15]):

$$\omega_k^2 = A_k B_k = \omega_{Hk}\left(\omega_{Hk} + \omega_M\right) + \omega_M^2 P\left(kd_\mathrm{f}\right)\left[1 - P\left(kd_\mathrm{f}\right)\right]. \tag{16}$$

In equation (15) we have neglected possible propagating-wave solutions $\mathbf{m}_{\mathrm{fk}} \propto \delta\left(\omega - \omega_k\right)$, which correspond to the continuous spin wave spectrum of the ferromagnetic film, because here we are interested in the standing spin wave excitations of a ferromagnetic stripe. Substituting expressions (15) for the magnetization components in equations (13*c*) and (13*d*) we get a coupled set of equations for the Fourier amplitudes of the spin excitations in the stripe:

$$-\mathrm{i}\omega m_{sn}^{x} = -\left(\omega_{Hn} + \omega_M\right) m_{sn}^{y} + \omega_M \sum_{n'=0}^{\infty}\left(P_{nn'} + S_{nn'}\right) m_{sn'}^{y} - \mathrm{i}\omega \sum_{n'=0}^{\infty} T_{nn'} m_{sn'}^{x} \tag{17a}$$

$$-\mathrm{i}\omega m_{sn}^{y} = \omega_{Hn} m_{sn}^{x} + \omega_M \sum_{n'=0}^{\infty}\left(P_{nn'} - S_{nn'}\right) m_{sn'}^{x} - \mathrm{i}\omega \sum_{n'=0}^{\infty} T_{nn'} m_{sn'}^{y} \tag{17b}$$

where the coupling coefficients $T_{nn'}$ and $S_{nn'}$ are given by

$$T_{nn'} = \frac{\omega_M^2}{2\omega}\frac{d_\mathrm{s} d_\mathrm{f}}{L}\int_{-\infty}^{\infty} Y_{kn}^{*} Y_{kn'} k^2 Q_k^2 \frac{\omega + \mathrm{sgn}\left(k\right)\Omega_k}{\omega_k^2 - \omega^2}\frac{\mathrm{d}k}{2\pi} \tag{18a}$$

$$S_{nn'} = \frac{\omega_M}{2}\frac{d_\mathrm{s} d_\mathrm{f}}{L}\int_{-\infty}^{\infty} Y_{kn}^{*} Y_{kn'} k^2 Q_k^2 \frac{\mathrm{sgn}\left(k\right)\omega + \Omega_k}{\omega_k^2 - \omega^2}\frac{\mathrm{d}k}{2\pi} \tag{18b}$$

and

$$\Omega_k \equiv \omega_{Hk} + \frac{\omega_M}{2}. \tag{19}$$

In the first approximation one can neglect coupling between the different standing dipolar spin wave modes of the stripe (modes with different index n). In this 'diagonal' case the approximate expression for the eigenfrequency ω_n of the stripe's standing spin wave mode can be written in a form similar to equation (16):

$$\left(1 - T_{nn}\right)^2 \omega_n^2 = \tilde{\omega}_{Hn}\left(\tilde{\omega}_{Hn} + \omega_M\right) + \omega_M^2 P_{nn}\left(1 - P_{nn}\right) \tag{20}$$

where

$$\tilde{\omega}_{Hn} \equiv \omega_{Hn} - \omega_M S_{nn}. \tag{21}$$

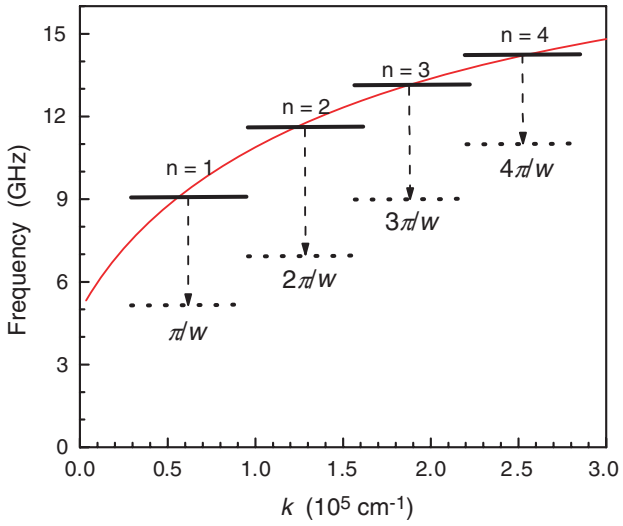

Figure 4. Frequency spectrum of standing spin wave modes $k_n = n\pi/w$ in a NiFe stripe calculated from equation (20). Solid horizontal lines correspond to the case of an isolated stripe with no coupling to the continuous sublayer ($S_{nn} = T_{nn} = 0$), while dashed horizontal lines correspond to the case of dipolar coupling between the stripe and the sublayer, when coupling coefficients are calculated from equation (18). The continuous solid line corresponds to the dispersion of a propagating spin wave in a continuous sublayer calculated from equation (16).

Note that the coupling coefficients $T_{nn'}$ and $S_{nn'}$ depend on the frequency $\omega = \omega_n$, and, therefore the diagonal dispersion equation (20) can be solved only numerically.

Equation (20) allows one to calculate the frequencies of spin wave modes in a structure consisting of an array of metal stripes above the continuous magnetic film of figure 1 in the case when all the geometric and material parameters of the structure are known. These parameters can be experimentally determined independently by measuring the dispersion law of the propagating spin wave mode (Damon–Eshbach mode) in the continuous film given by equation (16) and the frequency of the first ($p = 1$) exchange-dominated spin wave mode standing along the film thickness in a continuous film (perpendicular standing spin wave, PSSW) given by equation

$$\omega_p^2 = \left[\omega_H + \omega_M \alpha (p\pi/d_\mathrm{f})^2\right]\left[\omega_H + \omega_M \alpha (p\pi/d_\mathrm{f})^2 + \omega_M\right] \tag{22}$$

obtained from equation (12) in [16].

Comparison of equations (16) and (22) with the BLS experimental measurements made on the control sample of a continuous permalloy film with nominal thickness of 30 nm allowed us to determine the following parameters of the experimental structure figure 1: effective 'magnetic' thickness of permalloy layers $d_\mathrm{f} = d_\mathrm{s} = 26.5$ nm, saturation magnetization of permalloy film $4\pi M_\mathrm{s} = 10$ kOe, exchange constant of permalloy $A = 1 \times 10^{-6}$ erg cm^{-1}, and the gyromagnetic ratio $\gamma/2\pi = 3.0$ MHz Oe^{-1}.

Using these experimentally determined parameters and equation (20) we calculated the discrete spin wave frequencies in the isolated (no interaction with continuous film) array of permalloy stripes (shown by solid horizontal lines in figure 4) and the discrete spin wave frequencies in the array of permalloy stripes coupled to the continuous permalloy film through the non-magnetic spacer of the thickness $a = 10$ nm (shown by dashed horizontal lines in figure 4). The dispersion law of the surface spin wave mode (Damon–Eshbach mode) is shown in figure 4 by a solid continuous curve.

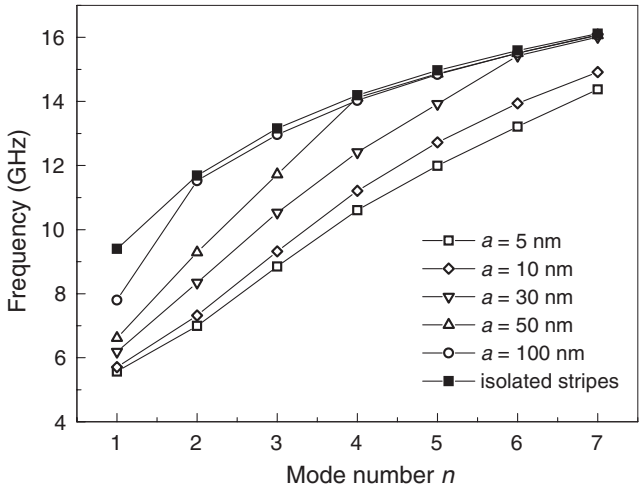

Figure 5. Dependences of the frequencies of standing spin wave modes on the mode number n calculated from equation (20) for the experimental structure shown in figure 1 for different values of thickness a of the Cu spacer.

It is clear from figure 4 that the dipole–dipole interaction between the stripes and the continuous film practically does not change the dispersion law of the propagating spin wave mode in the continuous film, but leads to a substantial reduction of frequencies of discrete spin wave modes standing along the stripe width (and having discrete wave numbers $k = n\pi/w$) in the array of magnetic stripes. To demonstrate that the frequency reduction is due to the strength of the dipolar coupling in figure 5 we present the results of calculation of the discrete spin wave mode frequencies of the stripes as a function of the mode number n for the different thicknesses of the Cu spacer in the range between 5 and 100 nm. It is clearly seen from figure 5 that the mode frequencies increase for the increasing the spacer thickness until they converge towards the values expected for isolated stripes.

4. Numerical model

We have also calculated the frequencies and spatial distributions of the discrete spin wave modes of the structure shown in figure 1 using the previously published numerical method [17] based on the Green function formalism for spin waves. This method involves calculation of magnetic correlation functions required for the fluctuation–dissipation theorem. In this numerical formulation we replaced the infinite permalloy sublayer used in the analytical model by a sublayer of a finite width (10 μm along the axis 'y') which was sufficiently wide to imitate a film of an infinitely large width in its interaction with a single magnetic stripe of width $w = 500$ nm. In order to reduce the number of calculation points, the sublayer was not meshed uniformly: the central part under the stripe (twice as large as the stripe) was meshed using triangular elements with the lateral size of about 10 nm (like in the stripe), while the remaining parts of the sublayer were meshed using triangular finite elements with a lateral size of about 50 nm. With such a mesh the calculated profiles of the discrete spin wave modes (shown in figure 6) demonstrated no significant discontinuity when crossing the boundaries between the two differently meshed zones.

The profiles of the eigenmodes were studied through the correlation function $\langle m_y(x, y), m_y(x', y')\rangle$. Letting $y = y'$ vary within the stripe ($-w/2 \leqslant y = y' \leqslant w/2$) and

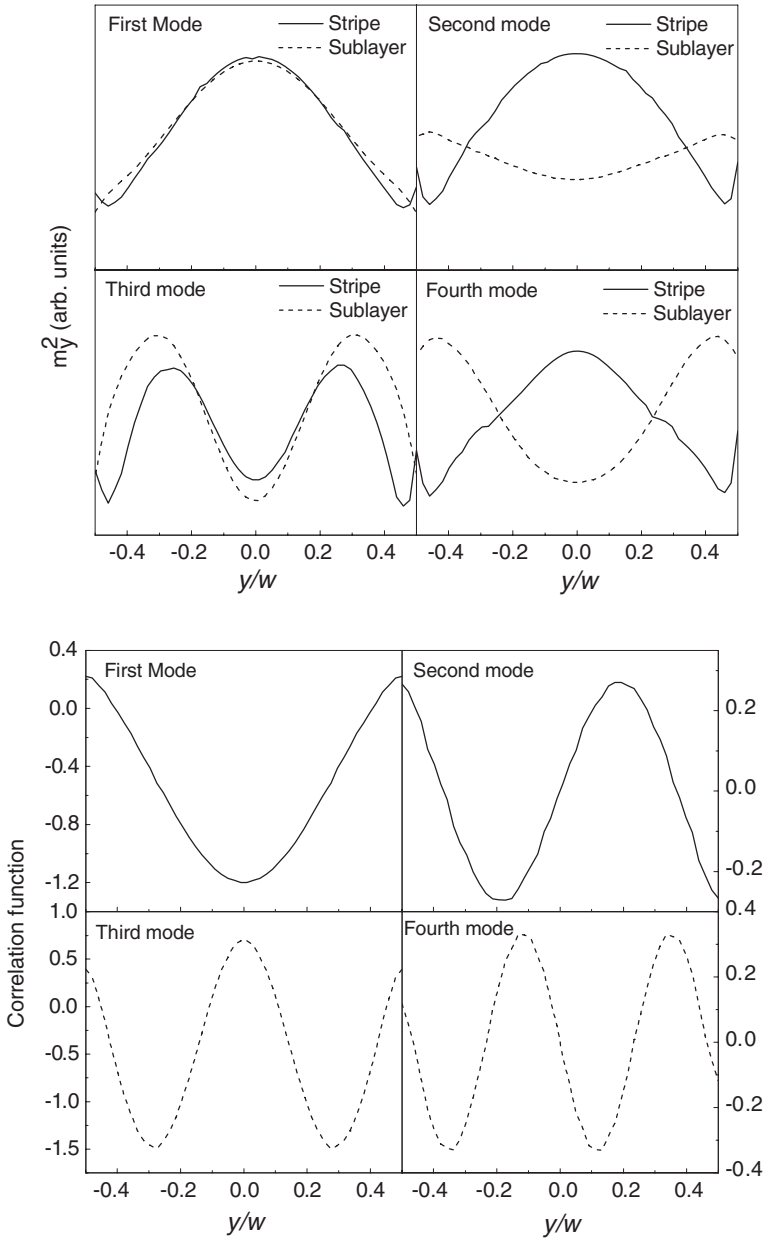

Figure 6. (Upper panel) Numerically calculated spatial profiles (squared dynamic magnetization as a function of the coordinate y) of the four lowest spin wave eigenmodes in the stripes and the sublayer under the stripe. (Lower panel) Calculated correlation functions for the same modes shown in the upper panel.

fixing $x = x' = d_s/2$ (stripe half-thickness), we obtain the profile within the stripe. Similarly, when $x = x' = d_f/2$ (sublayer half-thickness) we obtain the profile in the sublayer. Finally, by taking $y = y'$ within the stripe and x at the stripe mid-thickness and x' at the sublayer mid-thickness, we calculate the correlation function that characterizes the symmetry of the

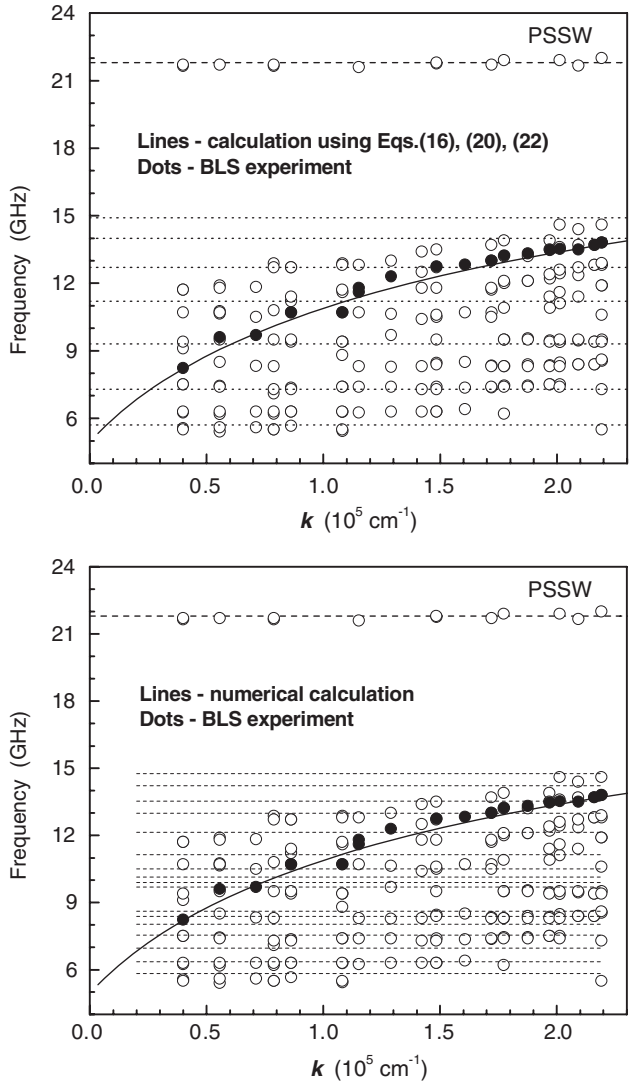

Figure 7. Comparison between the measured and calculated frequencies of spin wave modes in the structure shown in figure 1 as functions of the wave number component along the axis y. In the upper and lower panels the results of analytical (numerical) calculations are shown, respectively.

studied eigenmodes. Similar to the acoustic and optical mode assignment in a continuous unpatterned trilayer, consisting of two ferromagnetic films separated by a nonmagnetic spacer, the calculated modes can be primarily classified according to whether the precessional motion of the dynamic magnetizations in the two ferromagnetic layers is in phase or out of phase.

5. Results and discussion

The comparison between the experimentally measured frequencies of the spin wave modes in the structure shown in figure 1 (dots) and the results of analytic and numerical calculations of these frequencies (lines) are presented in the upper and lower panels of figure 7, respectively.

It is clear from the upper panel of figure 7 that the approximate analytic model equation (20) for $n = 1, 2, 3 \ldots$ gives a good quantitative description of all the 'odd-numbered' experimentally observed discrete modes of the structure shown in figure 1. At the same time, the 'even-numbered' experimentally observed spin wave modes are not described by the analytic model equation (20). We believe that this discrepancy between the experiment and our approximate analytic model is related to our initial assumption of a uniform distribution of the dynamic magnetization along the film thickness that was used in the analytic calculations leading to equation (20).

It is known, however, that in the geometry of figure 1 the spin waves propagating in the continuous sublayer are of a surface nature, and the distribution of the dynamic magnetization along the film thickness in such a wave is exponential and depends on the direction of wave propagation. In the case of a free magnetic film this fact does not influence the frequency of the waves and the waves propagating in both directions along the axis y have the same frequency due to the symmetry. This degeneracy is removed in the case when dipole–dipole interaction between the continuous sublayer and the magnetic stripe is present. In that case the quasi-Damon–Eshbach spin waves propagating in opposite directions along the axis y interact differently with the standing spin wave modes of a finite-width magnetic stripe, and two different characteristic frequencies appear in the experimental spectrum of the magnetic structure shown in figure 1 (see the experimental points in figure 7). Although our simplified analytical approach could not predict this frequency splitting, it explains the main qualitative feature produced by the dipole–dipole coupling between the continuous sublayer and the finite-width magnetic stripe, namely, the strong decrease of the frequencies of coupled modes in comparison with the case of isolated stripes (see figure 4).

In order to reproduce in a more quantitative way all the measured frequencies, we used the numerical method described in section 4. This enabled us to calculate both the discrete frequencies of the standing spin wave modes and spatial profiles of these modes along the stripe width (axis y). In figure 7 (bottom panel) we present the comparison between the BLS experiment and the numerically calculated frequencies of the spin wave modes. It is clear that numerical calculation describes the mode frequency splitting missed in the approximate analytic approach (top panel of figure 7) and gives a good quantitative description of the BLS experiment. In the upper panel of figure 6 we show the calculated spatial distributions of the dynamic magnetizations for the lowest four spin wave modes, while in the lower panel we report the correlation function for the same modes, also calculated numerically. As a general comment on the modes' profiles, we notice that the profiles are nearly the same in the stripe and in the sublayer just under the stripe for the first and third modes. Moreover, the correlation functions for these odd modes (lower panel of figure 6) are negative, indicating an out-of-phase precession, and are symmetric with respect to the mid-width of the stripe. In contrast, for the second and fourth modes, the profile in the stripe presents a maximum when the profile in the sublayer has a minimum. For these modes the correlation function is anti-symmetric with respect to the mid-width of the stripe, indicating a phase shift of $\pi/2$.

As a final step of our study, we investigated the behaviour of the frequencies of the spin wave modes (see the dots in figure 8) under the conditions of a magnetization reversal process in the structure figure 1 when the applied bias magnetic field was varied between -0.3 and $+0.3$ kOe. As can be inferred from the measured hysteresis loop shown in figure 2, in this field range there are two different possible magnetic configurations for the static magnetizations in the stripe and the continuous sublayer: parallel or antiparallel alignment. These different magnetization configurations affect the measured frequencies of spin wave modes in the structure shown in figure 1.

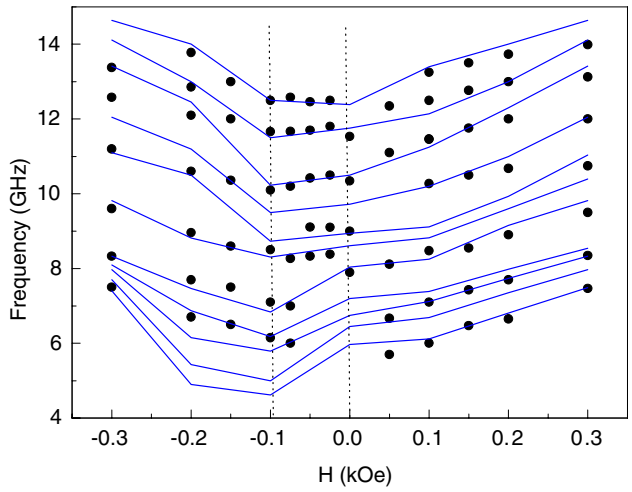

Figure 8. Comparison between the measured (dots) and numerically calculated (solid lines) spin wave mode frequencies of the structure shown in figure 1 as a function of H in the range from -0.3 to $+0.3$ kOe.

If we start from a positive applied field of $+0.3$ kOe and reduce it down to zero, the static magnetizations of the stripe and sublayer remain parallel to one another, and the mode frequencies show a monotonic decrease with the decrease of the bias magnetic field. As soon as the direction of the bias (and the direction of the static magnetization in a sublayer) is reversed, we see a plateau in the hysteresis loop in the range of negative bias fields between 0 and -100 Oe. In this range of the bias fields values the spin wave frequencies are also almost constant and independent of the exact value of the bias field. We note that no sharp discontinuity in the frequency values of spin wave modes is observed at the boundaries of this region. All these features are well reproduced in our numerical calculations (solid lines in figure 8).

6. Conclusions

In this paper we have demonstrated both experimentally and theoretically that the effect of dipole–dipole coupling between magnetic stripes of a finite width and a continuous magnetic sublayer leads to a significant reduction of the frequencies of the standing spin wave modes in the stripes, compared to the case of isolated magnetic stripes. In addition, one observes a splitting of the spin–wave peaks due to the dipole–dipole interaction of these modes with surface spin wave modes propagating in the continuous sublayer in two opposite directions (perpendicular to the direction of the in-plane bias magnetic field in this sublayer). The influence of reversing the relative magnetization directions in the stripe and in the sublayer has also been studied, showing that in the range of bias fields where these directions are opposite the spin wave frequencies are almost independent of the bias field magnitude.

Acknowledgments

This work was in part supported by the MURI grant W911NF-04-1-0247 from the Department of Defense of the USA, by the contract No. W56HZV-07-P-L612 from the US Army TARDEC, RDECOM, by the grant ECCS-0653901 from the National Science Foundation of the USA, and by the grant W911NF-04-1-0299 from the US Army Research Office.

References

[1] Demokritov S O and Hillebrands B 2002 *Spin Dynamics in Confined Magnetic Structures I* (*Springer Topics in Applied Physics* vol 83) ed B Hillebrands and K Ounadjela (Berlin: Springer) p 65 and references therein

[2] Gubbiotti G, Tacchi S, Carlotti G, Vavassori P, Singh N, Goolaup S, Adeyeye A O, Stashkevich A and Kostylev M 2005 *Phys. Rev.* B **72** 224413

[3] Gubbiotti G, Tacchi S, Carlotti G, Singh N, Goolaup S, Adeyeye A O and Kostylev M 2007 *Appl. Phys. Lett.* **90** 092503

[4] Gubbiotti G, Madami M, Tacchi S, Carlotti G and Okuno T 2006 *Phys. Rev.* B **73** 144430

[5] Chou K W, Puzic A, Stoll H, Schütz G, Waeyenberge B, Tyliszczak T, Rott K, Reiss G, Brückl H, Neudecker I, Weiss D and Back C H 2006 *J. Appl. Phys.* **99** 08F305

[6] Berkov D V and Gorn N L 2006 *Proc. Int. Conf. on Magnetism (Kyoto 2006)*

[7] Guslienko K Yu, Buchanan K S, Bader S D and Novosad V 2005 *Appl. Phys. Lett.* **86** 223112

[8] Gubbiotti G, Kostylev M, Sergeeva N, Conti M, Carlotti G, Ono T and Stashkevich A 2004 *Phys. Rev.* B **70** 224422

[9] Gubbiotti G, Carlotti G, Ono T and Roussigné Y 2006 *J. Appl. Phys.* **100** 023906

[10] Sergeeva N A, Chérif S M, Stashkevich A A, Kostylev M P and Ben Youssef J 2005 *J. Magn. Magn. Mater.* **288** 250

[11] Carlotti G and Gubbiotti G 2002 *J. Phys.: Condens. Matter* **14** 8199

[12] http://ghost.fisica.unipg.it

[13] Sandercock J R 1982 *Light Scattering in Solids III* ed M Cardona and G Güntherodt (Berlin: Springer) p 173

[14] Guslienko K Yu and Slavin A N 2005 *Phys. Rev.* B **72** 014463

[15] Damon R W and Eshbach J 1961 *J. Phys. Chem. Solids* **19** 309

[16] Demokritov S O, Hillebrands B and Slavin A N 2001 *Phys. Rep.* **348** 535

[17] Roussigné Y, Chérif S M and Moch P 2003 *J. Magn. Magn. Mater.* **263** 289